Article

Divalent Binding of a Bis(adamantyl)-Functionalized Calix[4]arene to β-cyclodextrin-based Hosts: An Experimental and Theoretical Study on Multivalent Binding in Solution and at Self-Assembled Monolayers

Alart Mulder, Tommaso Auletta, Andrea Sartori, Susanna Del Ciotto, Alessandro Casnati, Rocco Ungaro, Jurriaan Huskens, and David N. Reinhoudt

J. Am. Chem. Soc., **2004**, 126 (21), 6627-6636• DOI: 10.1021/ja0317168 • Publication Date (Web): 08 May 2004

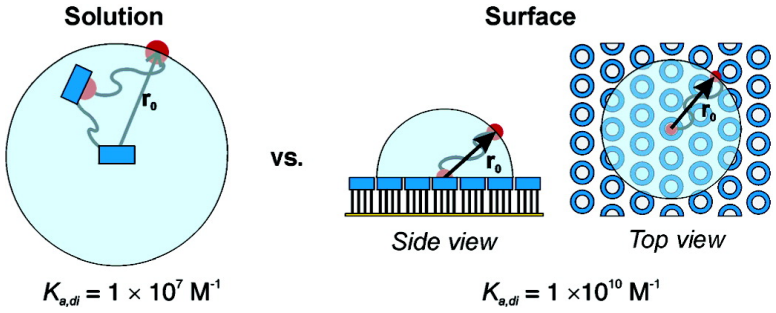

More About This Article

Additional resources and features associated with this article are available within the HTML version:

- Supporting Information
- Links to the 6 articles that cite this article, as of the time of this article download
- Access to high resolution figures
- Links to articles and content related to this article
- Copyright permission to reproduce figures and/or text from this article

View the Full Text HTML

J|A|C|S
ARTICLES
Published on Web 05/08/2004

Divalent Binding of a Bis(adamantyl)-Functionalized Calix[4]arene to β-cyclodextrin-based Hosts: An Experimental and Theoretical Study on Multivalent Binding in Solution and at Self-Assembled Monolayers

Alart Mulder,[†] Tommaso Auletta,[†] Andrea Sartori,[†,‡] Susanna Del Ciotto,[‡] Alessandro Casnati,[‡] Rocco Ungaro,[‡] Jurriaan Huskens,*[,†] and David N. Reinhoudt*[,†]

Contribution from the Laboratory of Supramolecular Chemistry & Technology, MESA+ Institute for Nanotechnology, University of Twente, P.O. Box 217, 7500 AE Enschede, The Netherlands and Dipartimento di Chimica Organica e Industriale, Università degli Studi di Parma, Parma, Italy

Received December 15, 2003; E-mail: j.huskens@utwente.nl; d.n.reinhoudt@utwente.nl

Abstract: The divalent binding of a bis(adamantyl)-functionalized calix[4]arene (**1**) to an EDTA-tethered β-cyclodextrin (CD) dimer (**2**) in solution (1.2×10^7 M^{-1}) was 3 orders of magnitude weaker than the binding constant ($\sim 10^{10}$ M^{-1}) for the interaction of **1** at CD self-assembled monolayers (SAMs) on gold. This difference in binding is rationalized using a theoretical model, which interprets the divalent binding as two consecutive monovalent binding events, i.e., an intermolecular interaction followed by an intramolecular binding event, the latter of which is associated with an effective concentration term accounting for the close proximity of the two interacting species. The methodology presented in the model is applicable to divalent binding both in solution and at SAMs and indicates that the difference in observed binding constants mainly stems from a difference in effective concentration.

Introduction

The use of supramolecular interactions for the positioning and/or immobilization of (bio)molecules at self-assembled monolayers (SAMs) is of high current interest.[1−8] SAMs of 2-aminoethanethiol hydrochloride have been used for the anchoring of crown ether-appended fullerenes[1] and cyclic peptides.[2] As these interactions are based on only one crown ether-cation interaction, the stability of these complexes is limited. This can be overcome by using the concept of multivalency—the simultaneous binding between multiple interlinked ligands on one side and multiple interlinked receptors on the other.[3] Tampé and co-workers used this approach for the immobilization of enzymes at SAMs by metal chelation.[4] More recently, adamantyl groups have been used to immobilize cytochrome C,[5] nanotubes,[6] dendrimers,[7,8] and dendritic wedges[8] at β-cyclodextrin (CD) SAMs by means of multiple hydrophobic interactions.

In principle, such supramolecular positioning allows controllable adsorption and desorption rates simply by tuning the number and type of interactions and therefore constitute a new paradigm for reversible and versatile nanofabrication schemes.[8] In this respect, supramolecular positioning can be superior to the more commonly used bio-affinity-based immobilization techniques that use antigen−antibody interactions or the biotin−avidin recognition motif, since the latter is very often quasi-irreversible, which means that control over the adsorption and especially the desorption rates is limited.[9,10] CDs are particularly attractive hosts as they are able to complex a variety of hydrophobic organic molecules in aqueous solutions with different binding affinities.[11]

[†] Laboratory of Supramolecular Chemistry & Technology, MESA+ Institute for Nanotechnology, University of Twente.

[‡] Dipartimento di Chimica Organica e Industriale, Università degli Studi di Parma.

(1) Arias, F.; Godinez, L. A.; Wilson, S. R.; Kaifer, A. E.; Echegoyen, L. *J. Am. Chem. Soc.* **1996**, *118*, 6086−6087.
(2) Miura, Y.; Kimura, S. *Langmuir* **1998**, *14*, 2761−2767.
(3) Mammen, M.; Choi, S.-K.; Whitesides, G. M. *Angew. Chem., Int. Ed.* **1998**, *37*, 2754−2794.
(4) (a) Dietrich, C.; Schmitt, L.; Tampé, R. *Proc. Natl. Acad. Sci. U.S.A.* **1995**, *92*, 9014−9018. (b) Thess, A.; Hutschenreiter, S.; Hofmann, M.; Tampé, R.; Baumeister, W.; Guckenberger, R. *J. Biol. Chem.* **2002**, *277*, 36 231−36 328.
(5) Fragoso, A.; Caballero, J.; Almirall, E.; Villalonga, R.; Cao, R. *Langmuir* **2002**, *18*, 5051−5054.
(6) Banerjee, I. A.; Yu, L.; Matsui, H. *J. Am. Chem. Soc.* **2003**, *125*, 9542−9543.
(7) Huskens, J.; Deij, M. A.; Reinhoudt, D. N. *Angew. Chem., Int. Ed.* **2002**, *41*, 4467−4471.
(8) Auletta, T.; Dordi, B.; Mulder, A.; Sartori, A.; Onclin, S.; Bruinink C. M.; Péter, M.; Nijhuis, C. A.; Beijleveld, H.; Schönherr, H.; Vancso, G. J.; Casnati, A.; Ungaro, R.; Ravoo, B. J.; Huskens, J.; Reinhoudt, D. N. *Angew. Chem., Int. Ed.*, **2004**, *43*, 369−373.
(9) For streptavidin and biotin: $K_a \approx 10^{15}$ M^{-1}; −21 kcal mol^{-1} (Green, N. M. *Methods Enzymol.* **1990**, *184*, 14−45). For the antibody−antigen interaction: K_a = up to 10^{14}; −19 kcal mol^{-1} (Portmann, A. J.; Levison, S. A.; Dandliker, W. B. *Immunochemistry* **1975**, *12*, 461−466).
(10) For an extensive review on binding affinities and the comparison of cyclodextrin-guest interactions with biomolecular interactions see: Houk, K. N.; Leach, A. G.; Kim, S. P.; Zhang, X. *Angew. Chem., Int. Ed.* **2003**, *42*, 4872−4897.
(11) For a general review on cyclodextrins see *Chem. Rev.* **1998**, *98*, volume 5. For a list with typical guest molecules see Rekharsky, M. V.; Inoue, Y. *Chem. Rev.* **1998**, *98*, 1880−1901.

For the successful design and application of multivalent ligands in nanofabrication at SAMs, a fundamental understanding of the multivalent interactions involved is crucial. Recently, Lees and co-workers published a general model for multivalent binding to rigid multivalent receptors.[12] Although this model was shown to give excellent correlations for a variety of multivalent model systems, its application is restricted to well-defined multivalent receptors with binding sites spaced at specific distances and thus this model is not readily applicable to multivalent binding at SAMs. Multivalent binding at SAMs can be very different from multivalent binding in solution. Previously, we qualitatively addressed the thermodynamic and kinetic issues related to the use of multiple interactions for stable surface attachment of adamantyl-functionalized dendrimers at CD SAMs.[7] This paper will present a quantitative study on the use of multiple hydrophobic interactions for the positioning of molecules on surfaces, and it discusses the simplest case of multivalency, i.e., a divalent interaction. The divalent binding of a bis-adamantyl-derivatized guest molecule with CD or a CD dimer in solution is compared to its binding at CD SAMs in order to resolve the current lack of understanding on multivalent interactions at surfaces.

Experimental Section

General. Chemicals were obtained from commercial sources and used as such. β-Cyclodextrin (CD) was dried in vacuo at 80 °C in the presence of P_2O_5 for at least 5 h before use. The syntheses of **2**,[13] **3**,[14] and **6**[15] have been reported previously. All solvents were dried according to standard procedures and stored over molecular sieves. All moisture sensitive reactions were carried out under a nitrogen atmosphere. NMR spectra were recorded on Bruker AC300 and AMX400 spectrometers. Spectra are reported in ppm downfield from TMS as an internal standard. Mass spectra by electrospray ionization (ESI) and chemical ionization (CI) methods were recorded on Micromass ZMD and Finnigan MAT SSQ710 spectrometers, respectively. FAB−MS spectra were recorded with a Finnigan MAT 90 spectrometer using *m*-NBA as a matrix. Melting points were determined with a Reichert melting point apparatus and are uncorrected. Elemental analyses were performed using a Carlo Erba EA1106. The presence of solvents in the analytical samples was confirmed by ^{1}H NMR spectroscopy. Analytical TLC was performed using Merck prepared plates (silica gel 60 F-254 on aluminum). Merck silica gel (40−63 μm) was used for flash chromatography.

(2-(2-(2-(2-(Adamantyl-1-oxy)ethoxy)ethoxy)ethoxy)ethanol (4). A solution of 1-bromoadamantane (10 g, 46.5 mmol) and triethylamine (1.96 mL, 139.5 mmol) in tetraethylene glycol (200 mL) was heated at 110 °C for 24 h. The mixture was allowed to cool to room temperature, 200 mL of CH_2Cl_2 were added, and the solution was washed with 1 M HCl (3 × 200 mL) and water (2 × 200 mL). The organic layer was dried over Na_2SO_4, and the solvent was evaporated under reduced pressure to give **4** as a slightly yellow oil. Yield 83%; ^{1}H NMR (300 MHz; $CDCl_3$): δ 3.71 (t, 2H, RC*H*$_2$OH, J = 4.9 Hz); 3.66−3.65 (m, 8H, ROC*H*$_2$CH_2OH); 3.61−3.56 (m, 6H, AdO(C*H*$_2$C*H*$_2$O)$_3$); 2.13 (bs, 3H, Ad[CH$_2$C*H*CH$_2$]); 1.74 (d, 6H, Ad[CHC*H*$_2$CH], J = 2.9 Hz); 1.61 (m, 6H, Ad[CHC*H*$_2$C]); ^{13}C NMR (75 MHz; $CDCl_3$): δ 72.6 (d, R*C*H$_2$OH); 72.3 (s, Ad[CH$_2$*C*CH$_2$]); 71.1, 70.5, 70.4, 70.1, 61.5, 59.1 (t, AdO(*C*H$_2$*C*H$_2$O)$_3$*C*H$_2$); 41.3 (t, Ad[C*C*H$_2$CH]); 36.3 (t, Ad[CH*C*H$_2$CH]); 30.4 (d, Ad[CH$_2$*C*HCH$_2$]); MS (CI) *m*/*z* (%): 329.1 (100) [M+H]$^+$; 327.2 (50) [M−H]$^+$. Anal. Calcd for $C_{18}H_{32}O_5$ (328.45): C, 65.82; H, 9.82. Found: C, 65.79; H, 9.86.

(2-(2-(2-(2-(Adamantyl-1-oxy)ethoxy)ethoxy)ethoxy)ethanol *p*-Toluenesulfonate (5). Compound **4** (7 g, 21.3 mmol) was dissolved in 80 mL of CH_2Cl_2. *p*-Toluenesulfonyl chloride (4.06 g, 21.3 mmol), Et_3N (2.95 mL, 21.3 mmol), and DMAP (100 mg) were added, and the solution was stirred overnight at room temperature. The mixture was quenched with 80 mL of 1 M HCl solution. The organic phase was washed with H_2O (2 × 80 mL), dried over Na_2SO_4 and evaporated under reduced pressure. The residue was purified by column chromatography (hexane/ethyl acetate, 1/1) to give the product **5** as a pale yellow oil. Yield 90%; ^{1}H NMR (300 MHz; $CDCl_3$): δ 7.79 (dd, 2H, Ar*H*, J_o=7.9 Hz, J_m=1.0 Hz); 7.34 (dd, 2H, Ar*H*, J_o=7.9 Hz, J_m=1 Hz); 4.16 (t, 2H, RC*H*$_2$OTs, J = 4.7 Hz); 3.69 (t, 2H, RC*H*$_2$CH$_2$OTs, J = 4.7 Hz); 3.63−3.56 (m, 12H, AdO(C*H*$_2$C*H*$_2$O)$_3$); 2.44 (s, 3H, ArC*H*$_3$); 2.13 (bs, 3H, Ad[CH$_2$C*H*CH$_2$]); 1.74 (d, 6H, Ad[CHC*H*$_2$CH], J = 2.8 Hz); 1.61 (m, 6H, Ad[CHC*H*$_2$C]); ^{13}C NMR (75 MHz; $CDCl_3$): δ 144.7 (s, Ar[*C*]S); 133.0 (s, Ar[*C*]CH$_3$); 129.7 (d, Ar[*C*]H); 127.9 (d, Ar[*C*]H); 72.2 (s, Ad[CH$_2$*C*CH$_2$]); 71.2, 70.7, 70.6, 70.5, 69.2, 68.6, 59.2 (t, AdO(*C*H$_2$*C*H$_2$O)$_4$); 41.4 (t, Ad[C*C*H$_2$CH]); 36.4 (t, Ad[CH*C*H$_2$CH]); 30.5 (d, Ad[CH$_2$*C*HCH$_2$]); 21.6 (q, Ar*C*H$_3$); MS (CI) *m*/*z* (%): 483.1 (100) [M+H]$^+$. Anal. Calcd for $C_{25}H_{38}O_7S_1$ (482.63): C, 62.22; H, 7.94. Found: C, 62.17; H, 7.99.

25,27-Bis(2-ethoxyethoxy)-26,28-bis(2-(2-(2-(2-(adamantyl-1-oxy)-ethoxy)ethoxy)ethoxy)ethoxy)-*p*-*tert*-butyl-calix[4]arene (7). Calix-[4]arene **6** (2.644 g, 3.33 mmol) was dissolved in 75 mL of dry DMF, and NaH (0.4 g, 10 mmol) was added. The solution, kept under a N_2 atmosphere, was stirred for 10 min before the addition of the tosylate **5** (4.823 g, 10 mmol). The mixture was heated at 75 °C for 48 h and then poured in 150 mL of 1 M aqueous HCl. The aqueous phase was extracted with CH_2Cl_2 (2 × 100 mL). The combined organic phases were washed with water (2 × 100 mL), dried over Na_2SO_4, and filtered, and the solvent was removed under vacuum. The residue was purified by column chromatography (hexane/diethyl ether/ethyl acetate, 1/1/1) to give **7** as a colorless oil. Yield: 90%; ^{1}H NMR (300 MHz; $CDCl_3$): δ 6.78 (s, 4H, Ar*H*); 6.74 (s, 4H, Ar*H*); 4.42 (d, 4H, ArC*H*$_2$Ar ax, J = 12.5 Hz); 4.10 (t, 4H, ArOC*H*$_2$; J = 5.7 Hz); 4.09 (t, 4H, ArOC*H*$_2$, J = 5.9 Hz); 3.94 (t, 4H, ArOCH$_2$C*H*$_2$; J = 5.7 Hz); 3.90 (t, 4H, ArOCH$_2$C*H*$_2$; J = 5.9 Hz); 3.68−3.56 (m, 28H, AdO(C*H*$_2$C*H*$_2$O)$_3$ + CH$_3$C*H*$_2$OR); 3.09 (d, 4H, ArC*H*$_2$Ar eq, J = 12.5 Hz); 2.13 (bs, 6H, Ad[CH$_2$C*H*CH$_2$]); 1.74 (d, 12H, Ad[CHC*H*$_2$C], J = 2.7 Hz); 1.60 (m, 12H, Ad[CHC*H*$_2$CH]), 1.22 (t, 6H, C*H*$_3$R, J = 6.9 Hz); 1.08 (s, 18H, ArC(C*H*$_3$)$_3$); 1.05 (s, 18H, ArC(C*H*$_3$)$_3$); ^{13}C NMR (75 MHz; $CDCl_3$): δ 153.4 (s, Ar ipso); 153.2 (s, Ar ipso); 144.5 (s, Ar para); 144.4 (s, Ar para); 133.8 (s, Ar ortho); 133.6 (s, Ar ortho); 124.9 (d, Ar meta); 124.9 (d, Ar meta); 73.0 (t, ArOC*H*$_2$); 72.9 (t, ArOC*H*$_2$); 72.1 (s, Ad[CH$_2$*C*CH$_2$]); 71.2, 70.61, 70.55, 70.4, 70.3, 69.6, 66.3 (t, AdOCH$_2$*C*H$_2$O(C*H*$_2$C*H*$_2$O)$_2$*C*H$_2$ + CH$_3$*C*H$_2$OC*H*$_2$); 59.2 (t, AdOC*H*$_2$); 41.4 (t, Ad[C*C*H$_2$CH]); 36.4 (t, Ad[CH*C*H$_2$CH]); 33.7 (s, Ar*C*(CH$_3$)$_3$); 31.4 (q, ArC(*C*H$_3$)$_3$); 31.0 (t, Ar*C*H$_2$Ar); 30.5 (t, Ad[CH$_2$*C*HCH$_2$]); 15.4 (q, R*C*H$_3$); MS (ESI+) *m*/*z* (%): 1435.7 (45) [M+Na]$^+$; 745.4 (90) [M+2K]$^{2+}$; 737.2 (100) [M+Na+K]$^{2+}$. Anal. Calcd for $C_{88}H_{132}O_{14}$ (1414.02): C, 74.75; H, 9.41. Found: C, 74.71; H, 9.46.

5,11,17,23-Tetranitro-25,27-bis(2-ethoxyethoxy)-26,28-bis(2-(2-(2-(adamantyl-1-oxy)ethoxy)ethoxy)ethoxy)ethoxy)calix[4]arene (8). Calix[4]arene **7** (0.5 g, 0.354 mmol) was dissolved in 5 mL of dry CH_2Cl_2, the solution was kept under N_2 and cooled to 0 °C. Glacial acetic acid (3.24 mL, 56.58 mmol) and 100% nitric acid (1.15 mL, 28.29 mmol) were added. The solution was stirred for 1.5 h, or until TLC (ethyl acetate) analysis of a sample indicated that the calix[4]-arene starting material had disappeared. The reaction mixture was slowly poured in 80 mL of saturated aqueous $NaHCO_3$ and extracted with CH_2Cl_2. The organic phase was washed with water (2 × 80 mL), dried

(12) Gargano, J. M.; Ngo, T.; Kim, Y.; Acheson, D. W. K.; Lees, W. J. *J. Am. Chem. Soc.* **2001**, *123*, 12 909−12 910.
(13) Michels, J. J.; Huskens, J.; Reinhoudt, D. N. *J. Am. Chem. Soc.* **2002**, *124*, 2056−2064.
(14) Beulen, M. W. J.; Bügler, J.; de Jong, M. R.; Lammerink, B.; Huskens, J.; Schönherr, H.; Vancso, G. J.; Boukamp, B. A.; Wieder, H.; Offenhäuser, A.; Knoll, W.; van Veggel, F. C. J. M.; Reinhoudt, D. N. *Chem. Eur. J.* **2000**, *6*, 1176−1183.
(15) Verboom, W.; Datta, S.; Asfari, Z.; Harkema, S.; Reinhoudt, D. N. *J. Org. Chem.* **1992**, *57*, 5394−5398.

over Na_2SO_4, and filtered, and the solvent was evaporated under reduced pressure. The residue was purified by column chromatography (EtOAc) to give **8** as a pale yellow oil. Yield: 65%; ^{1}H NMR (300 MHz; $CDCl_3$): δ 7.63 (s, 4H, Ar*H*); 7.52 (s, 4H, Ar*H*); 4.66 (d, 4H, ArCH_2-Ar ax, J = 14.0 Hz); 4.26 (t, 4H, ArOCH_2, J = 4.2 Hz); 4.20 (t, 4H, ArOCH_2, J = 4.3 Hz), 3.82 (t, 4H, ArOCH$_2$CH_2, J = 4.2 Hz); 3.75 (t, 4H, ArOCH$_2$CH_2, J = 4.3 Hz); 3.63−3.53 (m, 24H, AdO(CH_2CH_2O)$_3$); 3.48 (q, 4H, CH$_3$CH_2OR, J = 6.9 Hz); 3.36 (d, 4H, ArCH_2Ar eq, J = 14.0 Hz); 2.12 (bs, 6H, Ad[CH$_2$C*H*CH$_2$]); 1.71 (d, 12H, Ad[CHCH_2C], J = 2.7 Hz); 1.62 (m, 12H, Ad[CHCH_2CH]); 1.16 (t, 6H, CH_3CH$_2$OR, J = 6.9 Hz); ^{13}C NMR (75 MHz; $CDCl_3$): δ 161.7 (s, Ar ipso); 161.4 (s, Ar ipso); 142.9 (s, Ar para); 135.7 (s, Ar ortho); 135.4 (s, Ar ortho); 123.9 (d, Ar meta); 123.8 (d, Ar meta); 74.4 (t, ArO*C*H$_2$); 74.2 (t, ArO*C*H$_2$); 71.3 (s, Ad[CH$_2$*C*CH$_2$]); 70.6, 70.5, 70.4, 70.3, 69.4, 66.4 (t, AdOCH$_2$*C*H$_2$O(*C*H$_2$*C*H$_2$O)$_2$*C*H$_2$ + CH$_3$CH$_2$O*C*H$_2$); 59.2 (t, AdO*C*H$_2$); 41.4 (t, Ad[C*C*H$_2$CH]); 36.4 (t, Ad[CH*C*H$_2$CH]); 31.0 (t, Ar*C*H$_2$Ar); 30.4 (d, Ad[CH$_2$*C*HCH$_2$]); 15.2 (q, R*C*H$_3$); MS (ESI+) *m*/*z* (%): 1391.5 (100) [M+Na]$^+$; 707.6 (85) [M+2Na]$^{2+}$. Anal. Calcd for $C_{72}H_{96}O_{22}N_4$ (1369.57): C, 63.14; H, 7.07; N, 4.09. Found: C, 63.07; H, 7.14; N, 4.14.

5,11,17,23-Tetramino-25,27-bis(2-ethoxyethoxy)-26,28-bis(2-(2-(2-(adamantyl-1-oxy)ethoxy)ethoxy)ethoxy)ethoxy)calix[4]arene (9). Hydrazine monohydrate (1.79 mL, 57.3 mmol) and a catalytic amount of Pd/C were added to a solution of calix[4]arene **8** (0.982 g, 0.72 mmol) in 10 mL of absolute ethanol. The solution was stirred at 80 °C overnight. The mixture was cooled to room temperature, filtered, and evaporated to dryness. The residue was dissolved in 50 mL of ethyl acetate and washed with saturated aqueous $NaHCO_3$ (50 mL). The organic phase was dried with Na_2SO_4, filtered, and concentrated under reduced pressure, obtaining calix[4]arene **9** as a pale brown oil in a quantitative yield. ^{1}H NMR (300 MHz; $CDCl_3$): δ 6.08 (s, 4H, Ar*H*); 6.04 (s, 4H, Ar*H*); 4.32 (d, 4H, ArCH_2Ar ax, J = 13.2 Hz); 4.00 (t, 4H, ArOCH_2, J = 5.4 Hz); 3.99 (t, 4H, ArOCH_2, J = 5.8 Hz); 3.84 (t, 4H, ArOCH$_2$CH_2, J = 5.4 Hz); 3.79 (t, 4H, ArOCH$_2$CH_2, J = 5.8 Hz); 3.62−3.58 (m, 24H, AdO(CH_2CH_2O)$_3$); 3.53 (q, 4H, CH$_3$CH_2OR, J = 6.9 Hz); 2.90 (d, 4H, ArCH_2Ar eq, J = 13.2 Hz); 2.13 (bs, 6H, Ad[CH$_2$C*H*CH$_2$]); 1.74 (d, 12H, Ad[CHCH_2C], J = 2.7 Hz); 1.60 (m, 12H, Ad[CHCH_2CH]); 1.20 (t, 6H, CH_3CH$_2$OR, J = 6.9 Hz); ^{13}C NMR (75 MHz; $CDCl_3$): δ 149.2 (s, Ar ipso); 149.1 (s, Ar ipso); 140.1 (s, Ar para); 135.0 (s, Ar ortho); 134.9 (s, Ar ortho); 115.1 (d, Ar meta); 72.5 (t, ArO*C*H$_2$); 72.4 (t, ArO*C*H$_2$); 71.7 (s, Ad[CH$_2$*C*CH$_2$]); 70.7, 70.1, 69.9, 69.1, 65.8 (t, AdOCH$_2$*C*H$_2$O(*C*H$_2$*C*H$_2$O)$_2$*C*H$_2$ + CH$_3$CH$_2$O*C*H$_2$); 58.7 (t, AdO*C*H$_2$); 41.0 (t, Ad[C*C*H$_2$CH]); 35.9 (t, Ad[CH*C*H$_2$CH]); 30.5 (t, Ar*C*H$_2$Ar); 30.0 (d, Ad[CH$_2$*C*HCH$_2$]); 15.2 (q, *C*H$_3$); MS (MALDI-TOF) *m*/*z* (%): 1271.5 (100) [M+Na]$^+$; 1249.6 (60) [M+H]$^+$. Anal. Calcd for $C_{72}H_{104}O_{14}N_4$ (1249.64): C, 69.20; H, 8.39; N, 4.48. Found: C, 69.27; H, 8.30; N, 4.40.

5,11,17,23-Tetrakis[(*N*′,*N*″-bis-(*tert*-butyloxycarbonyl)guanidyl]-25,27-bis(2-ethoxyethoxy)-26,28-bis(2-(2-(2-(2-(adamantyl-1-oxy)-ethoxy)ethoxy)ethoxy)ethoxy)calix[4]arene (10). To a solution of tetraamine calix[4]arene **9** (0.553 g, 0.44 mmol) in 5 mL of dry DMF, kept under N_2, were added bis-BOC-thiourea (0.538 g, 1.95 mmol) and triethylamine (0.74 mL, 5.3 mmol). The solution was cooled to 0 °C, and $HgCl_2$ (0.529 g, 1.95 mmol) was added. After 4 h, the reaction was quenched by pouring diethyl ether (30 mL) in the flask and filtering the solution to remove the mercury salts. The solvent was removed under vacuum, and the residue was purified by column chromatography (ethanol) to give **10** as a colorless oil. Yield: 45%; ^{1}H NMR (300 MHz; $CDCl_3$): δ 11.62 (s, 4H, N*H*BOC); 9.86 (bs, 4H, ArN*H*); 6.97 (s, 4H, Ar*H*); 6.96 (s, 4H, Ar*H*); 4.48 (d, 4H, ArCH_2Ar ax, J = 13.2 Hz); 4.13 (t, 4H, ArOCH_2, J = 5.7 Hz); 4.10 (t, 4H, ArOCH_2, J = 5.9 Hz); 3.90 (t, 4H, ArOCH$_2$CH_2, J = 5.7 Hz); 3.82 (t, 4H, ArOCH$_2$CH_2, J = 5.9 Hz); 3.67−3.54 (m, 12H, AdO(CH_2CH_2O)$_3$); 3.49 (q, 4H, CH$_3$CH_2OR, J = 6.7 Hz); 3.17 (d, 4H, ArCH_2Ar eq, J = 13.2 Hz); 2.15 (bs, 6H, Ad[CH$_2$C*H*CH$_2$]); 1.76 (d, 12H, Ad[CHCH_2C] J = 2.4 Hz); 1.60−1.45 (m, 12H, Ad[CHCH_2CH]); 1.51 (s, 36H, BOC); 1.47 (s, 36H, BOC); 1.23 (t, 6H, CH_3R, J = 6.7 Hz); ^{13}C NMR (75 MHz; $CDCl_3$): δ 163.0 (s, *C*=O); 153.0 (s, Ar ipso); 152.5 (s, ArNH*C*); 134.1 (s, Ar para); 130.5 (s, Ar ortho); 122.7 (d, Ar meta); 82.5 (s, *C*(CH$_3$)$_3$); 78.6 (s, *C*(CH$_3$)$_3$); 72.7 (t, ArO*C*H$_2$); 72.6 (t, ArO*C*H$_2$); 71.6 (s, Ad[CH$_2$*C*CH$_2$]); 70.7, 70.1, 69.9, 69.6, 68.8, 65.8 (t, AdOCH$_2$*C*H$_2$O(*C*H$_2$*C*H$_2$O)$_2$*C*H$_2$ + CH$_3$*C*H$_2$O*C*H$_2$); 58.7 (t, AdO*C*H$_2$); 41.0 (t, Ad[C*C*H$_2$CH]); 35.9 (t, Ad[CH*C*H$_2$CH]); 30.7 (t, Ar*C*H$_2$Ar); 30.0 (d, Ad[CH$_2$*C*HCH$_2$]); 27.7 (q, R(*C*H$_3$)$_3$); 27.6 (q, R(*C*H$_3$)$_3$); 14.9 (q, R*C*H$_3$); MS (FAB −VE) *m*/*z* (%): 2217.6 (100) [M]$^-$; 2216.2 (80) [M−H]$^-$. Anal. Calcd for $C_{116}H_{176}O_{30}N_{12}$ (2218.75): C, 62.80; H, 8.00; N, 7.58. Found: C, 62.71; H, 8.10; N, 7.63.

5,11,17,23-Tetraguanidinium-25,27-bis(2-ethoxyethoxy)-26,28-bis(2-(2-(2-(2-(adamantyl-1-oxy)ethoxy)ethoxy)ethoxy)ethoxy)calix[4]-arene tetraacetate (1). Calix[4]arene **7** (0.232 g, 0.1 mmol) was dissolved in the minimum volume of diethyl ether (3 mL), and 2 M HCl solution in dioxane was added (1.83 mL, 3.66 mmol). The solution was stirred overnight at room temperature and then evaporated under reduced pressure. The residue was purified by column chromatography (*t*-BuOH/H_2O/CH_3COOH 6/2/1) to give **1** as a foam. The product was dissolved in water, filtered on microporosity filters (0.2 μm), and lyophilized, obtaining a white solid. Yield: 60%; Mp > 300 °C; ^{1}H NMR (300 MHz; CD_3OD): δ 6.67 (s, 4H, Ar*H*); 6.61 (s, 4H, Ar*H*); 4.62 (d, 4H, ArCH_2Ar ax, J = 13.6 Hz); 4.27 (t, 4H, ArOCH_2, J = 4.8 Hz); 4.18 (t, 4H, ArOCH_2, J = 4.9 Hz); 3.98 (t, 4H, ArOCH$_2$CH_2, J = 4.8 Hz); 3.92 (t, 4H, ArOCH$_2$CH_2, J = 4.9 Hz); 3.56−3.48 (m, 28H, AdO(CH_2CH_2O)$_3$ + CH$_3$CH_2OR); 3.27 (d, 4H, ArCH_2Ar eq, J = 13.6 Hz); 2.13 (bs, 6H, Ad[CH$_2$C*H*CH$_2$]); 1.94 (s, 12H, CH_3COO^-); 1.76 (d, 12H, Ad[CHCH_2C] J = 2.7 Hz); 1.67−1.60 (m, 12H, Ad-[CHCH_2CH]); 1.15 (t, 6H, CH_3CH$_2$OR, J = 6.9 Hz). ^{1}H NMR (300 MHz; D_2O): δ 6.67 (s, 4H, Ar*H*); 6.63 (s, 4H, Ar*H*); 4.44 (d, 4H, ArCH_2Ar ax, J = 13.6 Hz); 4.19 (bs, 4H, ArOCH_2); 4.13 (bs, 4H, ArOCH_2); 3.88 (bs, 4H, ArOCH$_2$CH_2); 3.61 (bs, 4H, ArOCH$_2$CH_2); 3.56−3.51 (m, 28H, AdO(CH_2CH_2O)$_3$ + CH$_3$CH_2OR); 3.26 (d, 4H, ArCH_2Ar eq, J = 13.6 Hz); 2.01 (bs, 6H, Ad[CH$_2$C*H*CH$_2$]); 1.79 (s, 12H, CH_3COO^-); 1.62 (bs, 12H, Ad[CHCH_2C]); 1.57−1.42 (m, 12H, Ad[CHCH_2CH]); 1.01 (t, 6H, CH_3CH$_2$OR, J = 6.9 Hz). ^{13}C NMR (75 MHz; CD_3OD): δ 156.1 (s, C=N); 155.9 (s, C=N); 155.2 (s, Ar ipso); 154.7 (s, Ar ipso); 136.0 (s, Ar para); 135.5 (s, Ar para); 128.6 (s, Ar ortho); 124.4 (d, Ar meta); 124.1 (d, Ar meta); 73.4 (t, ArO*C*H$_2$); 71.7 (s, Ad[CH$_2$*C*CH$_2$]); 70.3, 70.1, 69.8, 69.6, 69.2 (t, AdOCH$_2$*C*H$_2$O-(*C*H$_2$*C*H$_2$O)$_2$*C*H$_2$ + CH$_3$*C*H$_2$O*C*H$_2$); 58.5 (t, AdO*C*H$_2$); 40.7 (t, Ad[C*C*H$_2$CH]); 35.5 (t, Ad[CH*C*H$_2$CH]); 30.0 (d, Ad[CH$_2$*C*HCH$_2$]); 29.9 (t, Ar*C*H$_2$Ar); 13.9 (q, R*C*H$_3$). MS (MALDI-TOF) *m*/*z* (%): 1418.7 (100) [M-4CH_3COO^-−3H]$^+$. Anal. Calcd for $C_{84}H_{128}O_{22}N_{12}$ (1658.02): C, 60.85; H, 7.78; N, 10.14. Found: C, 60.93; H, 7.71; N, 10.06.

Adsorbate Synthesis and Substrates Preparation. Gold substrates were obtained from Ssens B. V. (Hengelo, The Netherlands). SAMs of **3** on Au(111) were prepared as reported previously.[19]

Calorimetric Titrations. Calorimetric measurements were carried out using a Microcal VP-ITC instrument with a cell volume of 1.4115 mL. For studying the complexation of **1** to native β-cyclodextrin (CD), 5 μL aliquots of 5−10 mM solution of CD were added to a 0.2−0.4 mM solution of **1** in the calorimetric cell, monitoring the heat change after each addition. For studying the complexation of **1** to the EDTA-dimer **2,** 5 μL aliquots of a 0.4 mM solution of **1** were added to a 0.05 mM solution of **2**. Dilution experiments showed that at the experimental concentrations employed here none of the species showed any detectable

(16) Lenferink, A. T. M.; Kooyman, R. P. H.; Greve, J. *Sens. Act. B* **1991**, *3*, 261−265.
(17) Beulen, M. W. J.; Bügler, J.; Lammerink, B.; Geurts, F. A. J.; Biemond, E. M. E. F.; van Leerdam, K. G. C.; van Veggel, F. C. J. M.; Engbersen, J. F. J.; Reinhoudt, D. N. *Langmuir* **1998**, *14*, 6424−6429.
(18) Schönherr, H.; Beulen, M. W. J.; Bügler, J.; Huskens, J.; van Veggel, F. C. J. M.; Reinhoudt, D. N.; Vancso, G. J. *J. Am. Chem. Soc.* **2000**, *122*, 4963−4967.
(19) de Jong, M. R.; Huskens, J.; Reinhoudt, D. N. *Chem. Eur. J.* **2001**, *7*, 4164−4170.

Scheme 1. Synthesis of Bis(adamantyl)-calix[4]arene **1**.

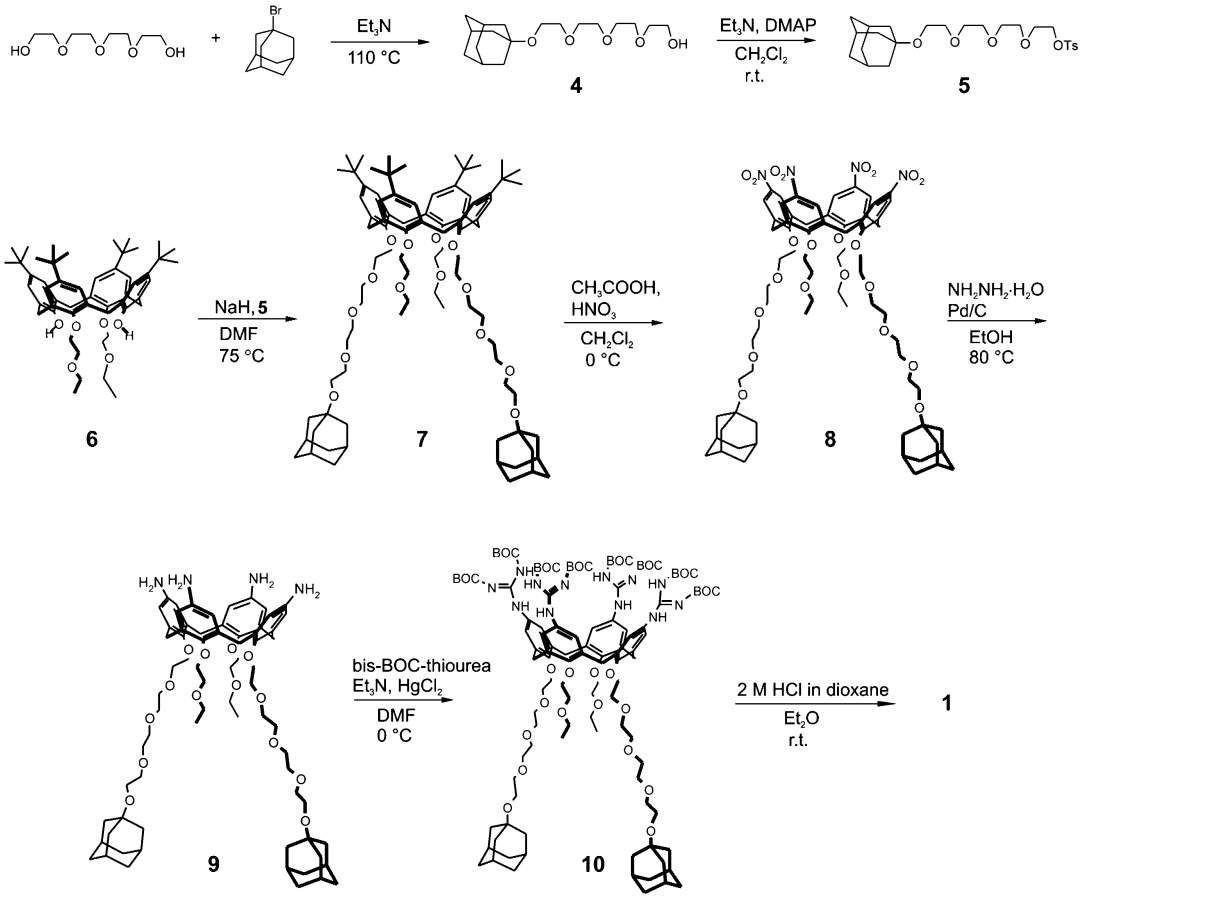

aggregation in water. All thermodynamic parameters given below are based on three independent calorimetric titrations.

SPR. SPR measurements were performed in a two-channel vibrating mirror angle scan setup based on the Kretschmann configuration, described by Kooyman and co-workers.[16] Light from a 2 mW HeNe laser is directed onto a prism surface by means of a vibrating mirror. The intensity of the light is measured by means of a large-area photodiode. This setup allows the determination of changes in plasmon angle with an accuracy of 0.0028. The gold substrate with the monolayer was optically matched to the prism using an index matching oil. A cell placed on the monolayer was filled with 800 μL of a CD solution (0.1, 0.5, 1.0, 2.5 or 5.0 mM). After stabilization of the SPR signal, titrations were performed by removing a known amount of CD solution and adding the same amount of a solution of **1** (1.05 μM) in the corresponding CD buffer. Between additions, the cell was cleaned by repeated washings (five times with a 10 mM CD solution), after which the solution was replaced with the initial CD solution. SPR measurements were repeated three times at each CD concentration.

Results and Discussion

Design of the Model System. As a model system to study multivalent interactions at SAMs we chose the interaction between an adamantyl-functionalized calix[4]arene (**1**) and a CD SAM of **3** on gold (Chart 1). Molecule **1** has been developed specifically for the interaction with CD SAMs. The calix[4]-arene is used as a synthetic platform and bears four guanidinium functionalities at the upper rim to increase water solubility. The lower rim is A−C bis-functionalized with adamantyl groups for the interaction with CD. Oligo(ethylene glycol) chains are used to space the two adamantyl groups in order to allow a

Chart 1. Guest and Host Compounds Used in This Study.

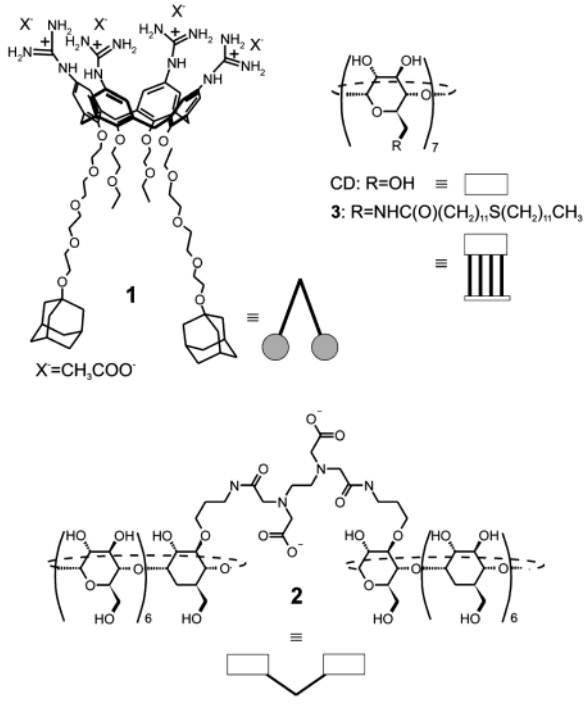

divalent interaction with CD SAMs, while retaining water-solubility and preventing nonspecific interactions.

As the adsorbate for the formation of the CD SAMs we used heptathioether-modified CD **3**.[14,17] These CD SAMs are particularly suited for this type of study for a number of reasons:

Table 1. Thermodynamic Parameters of the Complexation of **1** to CD and **2**, as Determined by ITC

host	stoichiometry (host:guest)	K (M^{-1})	$\Delta G°$ (kcal/mol)	$\Delta H°$ (kcal/mol)	$T\Delta S°$ (kcal/mol)
CD	2:1	$(4.6 \pm 0.3) \times 10^4$ [a]	-6.4 ± 0.1	-7.0 ± 0.5	-0.6 ± 0.6
2	1:1	$(1.2 \pm 0.1) \times 10^7$	-9.6 ± 0.1	-14.8 ± 0.5	-5.1 ± 0.6

[a] Intrinsic binding constant, K_i (see text and ref 25).

(i) The adsorbate forms densely and hexagonally packed, well-ordered SAMs[14,17] with a defined lattice constant;[18] (ii) Binding affinities at these SAMs can be studied with a variety of techniques such as electrochemical impedance,[14] surface plasmon resonance (SPR) spectroscopy,[14,19] and atomic force microscopy;[18,20] (iii) Simple, monovalent organic guests, such as adamantyl derivatives, show similar selectivities and binding strengths to such SAMs as to native CD in solution.[19] These allow the direct correlation between binding events in solution and at CD SAMs, which is advantageous for a fundamental understanding of multivalent binding on surfaces (see below). To correlate the multivalent nature of the binding of **1** at CD SAMs to binding in solution, the interactions of **1** with native CD and the divalent EDTA-based CD dimer **2**[13] were studied as well.

Synthesis. The synthesis of **1** is depicted in Scheme 1. 1-Adamantyl tetraethylene glycol **4** was synthesized by a nucleophilic substitution on 1-bromoadamantane with tetraethylene glycol in the presence of triethylamine, analogous to a previously reported procedure.[21] Tosylation of **4** gave the 1-adamantyl tetraethyleneglycol tosylate **5** which was reacted with 25,27-bis(2-ethoxyethoxy)-p-*tert*-butylcalix[4]arene (**6**)[22] at 75 °C in dry DMF using NaH as a base to give the bis-(adamantyl-tetraethylene glycol)-functionalized calix[4]arene. Under these conditions, **7** was obtained in the cone conformation. Substitution of the *tert*-butyl for nitro groups via an ipso-nitration reaction using glacial acetic acid and nitric acid gave tetranitro-calix[4]arene **8**. Low temperature and dry conditions are prerequisites for this reaction in order to prevent elimination of the adamantoxy groups under the strong acidic conditions used. Reduction of the nitro groups using hydrazine monohydrate and Pd/C in absolute ethanol gave the tetraamine calix-[4]arene **9** in nearly quantitative yield. Introduction of the BOC-protected guanidinium groups using bis-BOC-thiourea[23] was performed under the conditions reported by the group of Qian[24] and led to the formation of **10**. Initial attempts to deprotect the guanidinium groups using TFA led to the elimination of the adamantoxy groups. Selective removal of the BOC groups was achieved using 2 M HCl in dioxane, giving the desired product **1** as a tetrachloride salt. Purification of the product by column chromatography on SiO_2 using a *tert*-butyl alcohol/water/acetic acid mixture (6/2/1) as the eluent led to the exchange of the chloride counterions for acetate.

Binding in Solution. Binding studies with **1** in aqueous solution were performed using isothermal titration calorimetry (ITC). ITC measurements allow the direct determination of the association constant, K, and the binding enthalpy, $\Delta H°$, and thus provide a complete thermodynamic picture of the interactions under investigation. Calorimetric titrations were performed with CD and the EDTA-based CD dimer **2**[13] in order to get insight in the mono- and divalent binding behavior of **1** in solution, respectively. Figure 1 depicts the (exothermic) heat profiles obtained from the calorimetric titration of **1** with CD (top) and the titration of **2** with **1** (bottom).

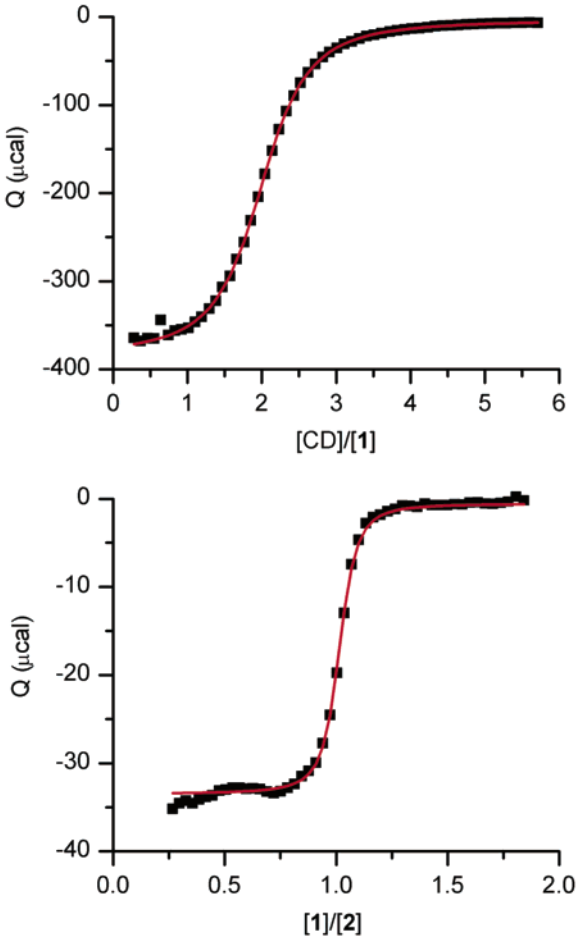

Figure 1. Heat evolved per injection plotted against the molar ratio and fits (solid lines) for the calorimetric titrations (25 °C) of CD (10 mM) to **1** (0.4 mM) (top) and of **1** (0.4 mM) to **2** (0.05 mM) (bottom) in water.

The inflection point in the titration curve obtained for the binding of **1** with CD indicates a 2:1 (host:guest) stoichiometry implying that **1** is bound by two CD cavities, one for each adamantane group. The curve was fitted to a 2:1 binding model (solid line, Figure 1, top), considering the two adamantyl groups as two identical independent binding sites and using the intrinsic association constant of a monovalent interaction, K_i, and its enthalpy of binding, $\Delta H_i°$, as independent fitting parameters.[25] The obtained thermodynamic parameters are listed in Table 1.

(20) Zapotoczny, S.; Auletta, T.; De Jong, M. R.; Schönherr, H.; Huskens, J.; van Veggel, F. C. J. M.; Reinhoudt, D. N.; Vancso, G. J. *Langmuir* **2002**, *18*, 6988−6994.
(21) Van Bommel, K. J. C.; Metselaar, G. A.; Verboom, W.; Reinhoudt, D. N. *J. Org. Chem.* **2001**, *66*, 5405−5412.
(22) Arduini, A.; Fanni, S.; Manfredi, G.; Ungaro, S.; Sicuri, A. R.; Ugozzoli, F. *J. Org. Chem.* **1995**, *60*, 1448.
(23) Iwanowicz, E. J.; Poss, M. A.; Lin, J. *Synth. Commun.* **1993**, *23*, 1443.
(24) Kim, K. S.; Qian, L. *Tetrahedron Lett.* **1993**, 34, 7677.

(25) For two independent, sequential binding events this implies: $K_1 = 2K_i$, $K_2 = {}^1/_2K_i$, and $\Delta H_1° = \Delta H_2° = \Delta H_i°$.

The intrinsic binding constant K_i of (4.6×10^4 M^{-1}) and the enthalpy of binding (−7.0 kcal/mol) are typical of a CD-adamantane interaction.[11] The observed 2:1 stoichiometry and the quality of the fit using independent binding sites (Figure 1, top) indicate that both adamantyl groups bind a CD cavity in a similar fashion, without interference between the two binding processes.

The titration curve for the titration of **2** with **1** (Figure 1, bottom) shows an inflection point at a molar ratio of 1, suggesting a 1:1 binding mode. Fitting of the titration curve with a 1:1 model and using the association constant and the binding enthalpy as independent fitting parameters gave thermodynamic parameters typical of a divalent interaction. The binding constant of 1.2×10^7 M^{-1} is orders of magnitude higher than the intrinsic binding constant for a single CD-adamantane interaction and the binding enthalpy, −14.8 kcal/mol, is twice the value found for the intrinsic binding enthalpy of **1** with CD (see Table 1). The strongly negative entropy of binding is attributed to restriction of mobility for both **1** and **2** caused by the divalent interaction. Dimer **2** did not show any evidence for self-inclusion of the rather hydrophilic EDTA tether into one of the CD cavities. Furthermore, the thermodynamic parameters obtained for the divalent binding of **1** to **2** imply that the interaction between **1** and **2** solely involves the two hydrophobic CD-adamantane interactions. Therefore, the overall divalent binding can be directly related to the intrinsic binding of **1** with native CD as determined with ITC (see Table 1) and can be well analyzed in terms of multivalency.[3]

Several approaches for the analysis of multivalent binding have been reported in the literature. Whitesides et al. proposed that multivalent binding should be analyzed in terms of entropy, assuming that the overall enthalpy of binding is the sum of the binding enthalpies of the individual ligands.[3,26] Alternatively, multivalent binding has been explained in terms of intrinsic binding constants and effective concentrations.[12,27,28] A general model for multivalent binding to rigid, multivalent receptors in solution based on the latter concept was recently published by Lees et al.[12] For ideal multivalent interactions, comprised of multiple, independent, and equal monotopic interactions, these two binding models are basically similar. In principle, both approaches seem equally well applicable to the interaction between **1** and **2**; as stated above, the enthalpy of binding found for the interaction between **1** and **2** is the sum of the enthalpy of the binding of two CD-adamantane interactions (see Table 1) and the divalent binding is directly related to an intrinsic monovalent binding. However, the correct interpretation of the entropy term for multivalent interactions is far from trivial.[26] Moreover, when studying binding of guests at CD SAMs, only stability constants are readily accessible. Therefore, for our study, the latter approach, which is based on intrinsic binding constants, is more easily applicable.

As illustrated for the binding of **1** by **2** in Figure 2, the divalent binding can be considered to consist of two independent, sequential binding events, and the overall binding process can be described in terms of two single host−guest (CD-adamantane) interactions. As stated above, these sequential interactions are directly related to the intrinsic binding constant

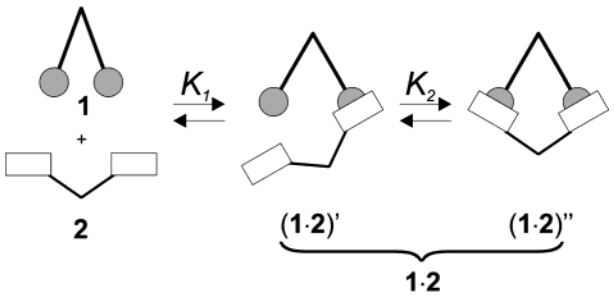

Figure 2. Equilibria for the sequential binding of **1** to **2**.

of the individual host−guest interaction, i.e., as determined for **1**-CD_2. The first, intermolecular, interaction can be directly related to the intrinsic binding constant ($K_1 = 4K_i$). The second, *intramolecular*, interaction is the product K_i and an effective concentration term (C_{eff}), which accounts for the uncomplexed host (CD) concentration experienced by the uncomplexed guest (adamantyl group) ($K_2 = {}^1/_2 C_{eff} K_i$). The term effective concentration is used to differentiate between inter- and intramolecular reactions and interactions, and accounts for the close proximity of two reactive or complementary species in an intramolecular reaction or binding event.[29] The effective concentration represents a probability of interaction between the two reactive or complementary species, and is conceptually similar to the more generally used term effective molarity (EM),[30,31] which represents the ratio of rate or association constants for intra- and intermolecular processes.[31,32] The effective concentration symbolizes a "physically real" concentration of one of the reacting or interacting species as experienced by its complementary counterpart.[27−29,31]

The overall binding constant for a divalent interaction in solution consisting of two identical, independent binding processes can thus be expressed in terms of the effective concentration and the intrinsic binding constant using eq 1.

$$K = 2C_{eff}(K_i)^2 \tag{1}$$

On the basis of the intrinsic binding constant determined for **1**·$(CD)_2$, $K_i = 4.6 \times 10^4$ M^{-1}, and the binding constant of **1·2**, $K = 1.2 \times 10^7$ M^{-1}, an experimental C_{eff} of 2.8 ± 0.6 mM is calculated.

A theoretical estimate for C_{eff} can be obtained using the well-known formula for cyclization probability, eq 2.[29,33−35]

$$C_{eff} = \frac{1}{N_{AV}}\left(\frac{3}{(2\pi\bar{r}_0^{\,2})}\right)^{3/2} \tag{2}$$

Here, N_{AV} is Avogadro's number, and $\bar{r}_0$ is the root-mean-square

(26) Rao, J.; Lahiri, J.; Weis, R. M.; Whitesides, G. M. *J. Am. Chem. Soc.* **2000**, *122*, 2698−2710.
(27) Kramer, R. H.; Karpen, J. W. *Nature*, **1998**, *395*, 710−713.
(28) Kitov, P. I.; Shimizu, H.; Homans, S. W.; Bundle, D. R. *J. Am. Chem. Soc.* **2003**, *125*, 3284−3294.
(29) Winnik, M. A. *Chem. Rev.* **1981**, *81*, 491−524.
(30) For the concept of EM applied to reaction kinetics see for example: (a) Kirby, J. A. *Adv. Phys. Org. Chem.* **1980**, *17*, 183−278. (b) Galli, C.; Mandolini, L. *Eur. J. Org. Chem.* **2000**, 3117−3125. For the concept of EM applied to self-assembly in solution see for example: (c) Ercolani, G. *J. Phys. Chem. B.* **2003**, *107*, 5052−5057.
(31) Mandolini, L. *Adv. Phys. Org. Chem.* **1986**, *22*, 1−111.
(32) C_{eff} follows from geometrical and probability considerations and therefore always represents a physically real concentration. In contrast, EM is an empirical parameter derived from the ratio of stability or rate constants for intra- and intermolecular binding events. Particularly when derived from rate constants, EM values have in some cases been observed to be extremely high (up to 10^8 M), clearly not a physically real concentration (see refs 30 and 31). When binding is reversible and statistical (i.e. when dealing with independent binding sites), C_{eff} and EM should be equal. Therefore, for clarity, the term C_{eff} is also used in this manuscript for those cases where the effective concentration is calculated from the observed and intrinsic binding constants.

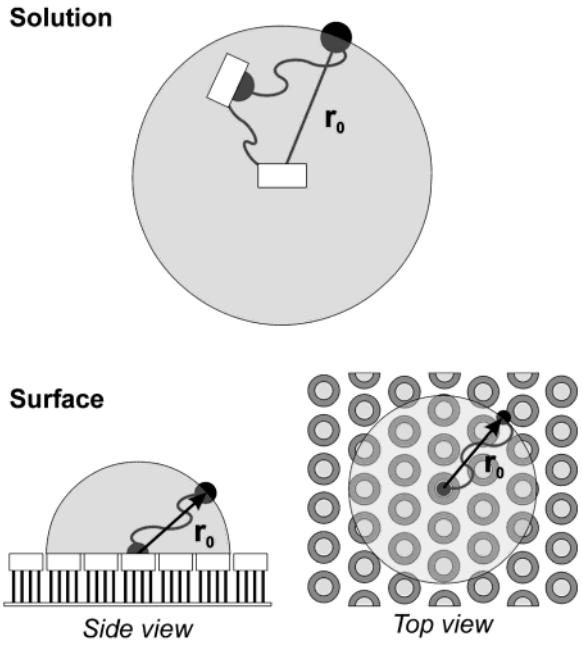

Figure 3. Schematical representation of the concept of C_{eff} for the interaction between **1** and **2** (top) and of **1** to CD SAMs (bottom).

distance between the two ends of the chain. Equation 2 is based on Gaussian probability functions and random walk statistics,[33,34] and gives the probability for the presence of two interlinked chain ends within an infinite small volume. It shows that C_{eff} has an inverse cubic relation to $\bar{r}_0$.

A crude approximation of C_{eff}, which is also applicable to CD SAMs (see below), can be made by considering the number of available receptor sites within the probing volume of the uncomplexed guest (Figure 3, top).[27,31] The radius of the probing volume is defined by the average end-to-end distance between the uncomplexed ligand (adamantane) and the free receptor sites (CD cavities). Here, it is assumed that the probability of an interaction between the two species is uniformly distributed within this volume. For a divalent binding in solution C_{eff} is therefore given by eq 3. [27,31,36]

$$C_{eff} = \frac{3}{4\pi\bar{r}_0^{\,3}N_{AV}} \qquad (3)$$

Comparison of eqs 2 and 3 shows that the approximation of C_{eff} as given by eq 3 differs a prefactor $(\pi/6)^{1/2}$ (= 0.72) from eq 2. This factor is within experimental error of accessible C_{eff} values (see above) and within the range of possible C_{eff} values based on $\bar{r}_0$ (see below). Furthermore, in the case of the modeling of binding to CD SAMs, which is our prime objective, it will be shown that K_i values obtained using this model are fairly insensitive to the value of C_{eff} (see below).

(33) Kuhn, W. *Kolloid Z.* **1934**, *68*, 2−15.
(34) Jacobson H.; Stockmayer, W. H. *J. Phys. Chem.* **1950**, *18*, 1600−1606.
(35) An alternative way to estimate C_{eff} is given in ref 30b, employed for macrocyclizations: from their Table 1, and noting that the number of rotatable bonds in the complex **1**·**2** is approximately 50, follows that C_{eff} is expected to be 9 mM (when corrected for the statistical factor 2 higher probability of ring-opening in our divalent complex).
(36) This concept has also been applied successfully to the pentavalent binding to toxins. (a) Fan, E.; Zhang, Z.; Minke, W. E.; Hou, Z.; Verlinde, C. L. M. J.; Hol, W. G. J. *J. Am. Chem. Soc.* **2000**, *122*, 2663−2664. (b) Merrit, E. A.; Zhang, Z.; Pickens, J. C.; Ahn, M.; Hol, W. G. J.; Fan, E. *J. Am. Chem. Soc.* **2002**, *124*, 8818−8824.

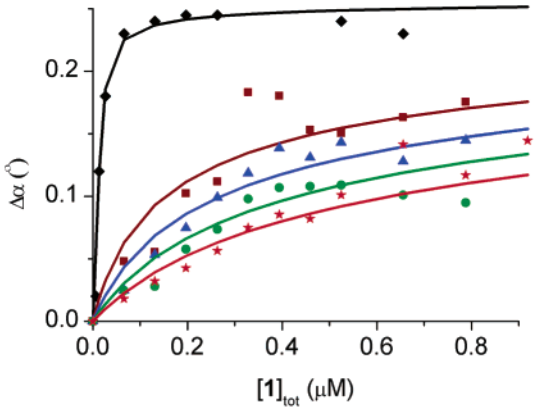

Figure 4. SPR titrations (data points) and corresponding fits for the sequential binding model (solid lines) for different titrations of **1** to CD SAMs at five different CD concentrations in solution (◆ = 0.1 mM; ■ = 0.5 mM; ▲ = 1 mM; ●, = 2.5 mM; ★ = 5 mM). Errors on the data points are approximately 0.02°.

An estimate for the average root-mean-square end-to-end distance, $\bar{r}_0$, was obtained using three-dimensional random walk statistics (see the Supporting Information) which gave values for C_{eff} ranging from 1.8 to 92.0 mM. The experimentally determined C_{eff} of 2.8 mM is within this range of calculated theoretical C_{eff} values. The relatively low value for the experimentally determined C_{eff} may imply that the rotational mobility within complex (**1**·**2**)′ is rather limited.

This result suggests that the concept, where the divalent binding of **1** and **2** is considered to consist of two sequential binding steps, is viable and that C_{eff}, approximated by considering the physically real available host sites within the probing volume of the uncomplexed guest, can be used to account for the difference between the intra- and intermolecular interactions.

Binding at the Surface. The binding of **1** to CD SAMs was studied by surface plasmon resonance spectroscopy (SPR). Figure 4 shows five SPR titration curves performed at different CD buffer concentrations. The SPR curves were obtained by the addition of increasing amounts of a 1 μM solution of **1** to a CD solution on top of a CD SAM. Additions of **1** resulted in an increase of the SPR angle, indicative of adsorption. The adsorption was followed for 200 s after which the surface was regenerated by repeatedly rinsing the cell with 10 mM CD to obtain complete restoration of the SPR signal, indicating the desorption of **1** from the surface.

The interaction of **1** with CD SAMs was studied at different concentrations of CD in solution in order to test the influence of competition between CDs in solution and the CDs of the SAM. CD concentrations in solution higher than 0.1 mM were required in order to obtain reliable binding constants. As can be seen in Figure 4, titration of **1** at 0.1 mM gives nearly quantitative adsorption, and leads to the depletion of **1** from solution for the first few data points. Therefore, titrations at higher CD concentrations were needed. The decreasing slopes of the binding curves at increasing CD concentration indicate that the CD in solution competes with the CD sites at the surface.

Titrations performed with **1** on 11-mercapto-1-undecanol reference SAMs only gave a small concentration effect on the SPR signal, which could be easily restored by washing the SAMs with water. No binding curves could be recorded, indicating the absence of specific interactions between **1** and the reference SAMs. SPR titrations at CD SAMs performed in

Table 2. Binding Constants for the Interaction of **1** with CD SAMs

$[CD]_{sol}$ (mM)	K_{LM}[a] (M^{-1})	$K_{i,s}$[b] (M^{-1})
0.1	1.7×10^{10}	3.3×10^{5}
0.5	2.8×10^{9}	1.1×10^{5}
1.0	6.4×10^{9}	1.6×10^{5}
2.5	2.8×10^{10}	3.1×10^{5}
5	7.9×10^{10}	5.1×10^{5}

[a] Langmuir fit to a 1:1 model; [b] Fit to the multivalency model, using $C_{eff,max} = 0.2$ M.

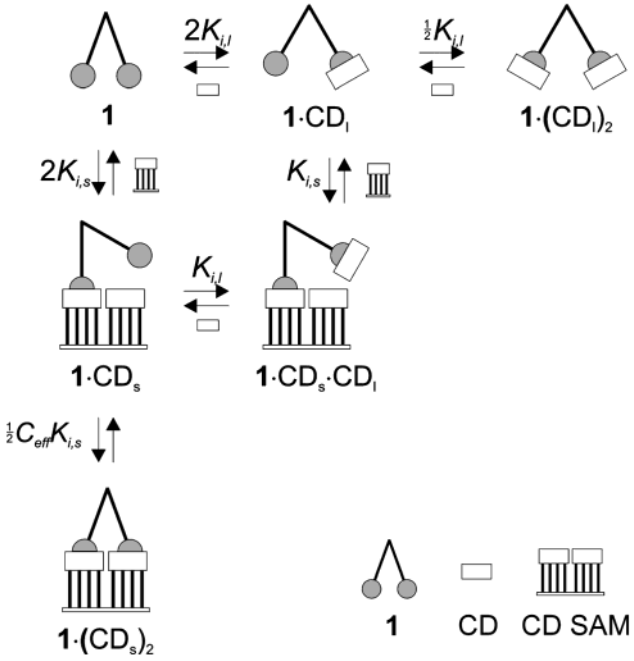

Figure 5. Equilibria for the sequential binding of **1** to CD SAMs.

the presence of 0.1 M KCl gave binding curves similar to those obtained without a background electrolyte, indicating that possible electrostatic repulsion at the monolayer can be neglected.

The titration curves could be fitted well to Langmuir isotherms using a model representing a single binding event in which it was assumed that both adamantyl moieties of **1** simultaneously interact with a CD cavity at the surface.[37] Using the binding constants for the interaction of **1** with the competing CD in solution as determined by ITC (see above), each binding curve of Figure 4 was satisfactory fitted giving complexation constants K_{LM} ranging from 2.8×10^{9} to 7.9×10^{10} M^{-1} (see Table 2). The obtained binding constants for the divalent binding of **1** at CD SAMs are 2 to 3 orders of magnitude higher compared to the binding constant found for the divalent binding of **1** to **2** in solution (1.2×10^{7} M^{-1}, see above). Such large differences between divalent binding in solution and at SAMs are not uncommon and have been observed before.[38,39] Here, we show that these differences in binding affinity found for the divalent interaction in solution and at surfaces can be rationalized when interpreted as 2 sequential binding events, using the effective concentration concept, as will be discussed below.

Figure 5 depicts the possible routes for the sequential divalent binding of **1** to CD SAMs and the equilibria involved. The equilibria contain solution (top row) and surface species (lower two rows) and they describe the interaction of **1** with CDs in solution (CD_l; from left to right) and with CDs at the surface (CD_s; from top to bottom). As for the sequential binding in solution, the sequential binding events at the surface are considered equal and independent. Consequently, all binding constants can be expressed in terms of intrinsic binding constants, here taken separately for binding to a solution host ($K_{i,l}$) and a surface host ($K_{i,s}$), similarly as described above for the binding of **1** to **2** in solution. For $K_{i,l}$ the value as determined above using ITC for the binding of **1** and CD in solution is used (4.6×10^{4} M^{-1}). It is assumed to hold for the binding of a surface-confined guest as well (Figure 5, equilibrium in second row). Consequently, the equilibria expressed in rows can be expressed in terms of $K_{i,l}$.

The first binding constant of **1** with the CD SAM is given by eq 4.[40]

$$\frac{[\mathbf{1} \cdot CD_s]}{[\mathbf{1}][CD_s]} = 2K_{i,s} \qquad (4)$$

The equilibrium is expressed in terms of the free, surface-confined host concentration in the total sample volume, $[CD_s]$ (in M). In principle, it is also possible to express the equilibrium in terms of absolute or relative surface coverages, however, the use of $[CD_s]$ simplifies the solving of the mass balances as shown below.

The second, intramolecular binding event at the surface, the formation of $\mathbf{1}\cdot(CD_s)_2$, is accompanied by an effective concentration term, C_{eff}, similar to the second binding event for the sequential divalent binding of **1** in solution. C_{eff} represents the effective concentration of *free* host sites at the surface and is thus surface coverage-dependent. This is accounted for by multiplying the maximum effective concentration, $C_{eff,max}$, which is the number of accessible host sites in the probing volume (see Figure 3, bottom, and see below), with the fraction of free host sites at the surface ($= [CD_s]/[CD_s]_{tot}$) giving eq 5.

$$\frac{[\mathbf{1} \cdot (CD_s)_2]}{[\mathbf{1} \cdot (CD_s)]} = {}^{1}/_{2} C_{eff,max} \frac{[CD_s]}{[CD_s]_{tot}} K_{i,s} \qquad (5)$$

In our model, $K_{i,s}$ is optimized as a fitting parameter independently of the fixed value of $K_{i,l}$. The optimized value of $K_{i,s}$ is then compared to previously obtained intrinsic binding constants for the complexation of monovalent adamantyl derivatives at SAMs of **3** in the evaluation of the data.

Combination of the equilibrium constant definitions with the mass balances for [**1**], $[CD_l]_{tot}$ and $[CD_s]_{tot}$ gives the numerically solvable eqs 6−8 in which the only two unknown parameters are $K_{i,s}$ and $C_{eff,max}$.

(37) All titration curves were fitted in a least-squares optimization simultaneously with one value for the maximum SPR response ($\Delta\alpha_{max}$) but individually adaptable K_{LM} or $K_{i,s}$ values. The Langmuir fits (not shown) are by eye indistinguishable from the fits to the sequential binding model as given in Figure 4. Fits with independently varied $\Delta\alpha_{max}$ values gave a similar spreading in K_{LM} or $K_{i,s}$ values.

(38) Major, R. C.; Zhu, X. Y. *J. Am. Chem. Soc.* **2003**, *123*, 8454−8455.

(39) (a) Rao, J.; Yan, L.; Xu. B.; Whitesides, G. M. *J. Am. Chem. Soc.* **1999**, *121*, 2629−2630. (b) Rao, J.; Yan, L.; Lahiri, J.; Whitesides, G. M.; Weis, R. M.; Warren, H. S. *Chem. Biol.* **1999**, *6*, 353−359.

(40) The statistical factor for the first interaction at the surface is 2 as it accounts for the interaction of a divalent guest molecule with a single host site at the surface.

$$[\mathbf{1}]_{tot} = [\mathbf{1}] + [\mathbf{1}\cdot CD_l] + [\mathbf{1}\cdot (CD_l)_2] + [\mathbf{1}\cdot CD_s] + [\mathbf{1}\cdot CD_l\cdot CD_s] + [\mathbf{1}\cdot (CD_s)_2] =$$

$$[\mathbf{1}] + 2K_{i,l}[\mathbf{1}][CD_l] + K_{i,l}{}^2[\mathbf{1}][CD_l]^2 + 2K_{i,s}[\mathbf{1}][CD_s] + 2K_{i,l}K_{i,s}[\mathbf{1}][CD_l][CD_s] + K_{i,s}{}^2[\mathbf{1}][CD_s]^2\frac{C_{eff,max}}{[CD_s]_{tot}} \quad (6)$$

$$[CD_l]_{tot} = [CD_l] + [\mathbf{1}\cdot CD_l] + 2[\mathbf{1}\cdot (CD_l)_2] + [\mathbf{1}\cdot CD_l\cdot CD_s] =$$

$$[CD_l] + 2K_{i,l}[\mathbf{1}][CD_l] + 2K_{i,l}{}^2[\mathbf{1}][CD_l]^2 + 2K_{i,l}K_{i,s}[\mathbf{1}][CD_l][CD_s] \quad (7)$$

$$[CD_s]_{tot} = [CD_s] + [\mathbf{1}\cdot CD_s] + [\mathbf{1}\cdot CD_l\cdot CD_s] + 2[\mathbf{1}\cdot (CD_s)_2] =$$

$$[CD_s] + 2K_{i,s}[\mathbf{1}][CD_s] + 2K_{i,l}K_{i,s}[\mathbf{1}][CD_l][CD_s] + 2K_{i,s}{}^2[CD_s]^2\frac{C_{eff,max}}{[CD_s]_{tot}}[\mathbf{1}] \quad (8)$$

Analogous to the binding in solution, $C_{eff,max}$ can be estimated by considering the number of accessible host sites in the probing volume of the uncomplexed adamantyl moiety of $\mathbf{1}\cdot CD_s$, which in this case is constituted of a hemisphere with radius $\bar{r}_0$ (see Figure 3, bottom). On the basis of the common formula for cyclization probability (eq 2), Lees et al. developed an expression for the calculation of a maximally attainable C_{eff} for rigid multivalent hosts, in which the host sites are spaced by a *specific* distance, in combination with ideal multivalent guests, having an *optimal* spacing between the individual ligand sites.[29] Our CD SAMs consist of an infinite number of bindings sites and, depending on the spacer length between the two adamantyls, there are multiple possible binding sites spaced at multiple possible distances that enable a divalent binding. Therefore, the calculation of C_{eff} as proposed by Lees et al. is not readily applicable to the interaction of **1** at the CD SAMs. Instead, the method used for the approximation of C_{eff} in solution offers a viable alternative for the approximation of $C_{eff,max}$ at surfaces as well.

The methodology used for the approximation of $C_{eff,max}$ at the surface is similar to that used for the approximation of C_{eff} in solution, with the exception that the number of available CD sites at the surface exceeds 1 and is dependent on the root-mean-square end-to-end distance, $\bar{r}_0$. Application of the concept of effective concentration to CD SAMs leads to eq 9 (for derivation see Supporting Information) in which A_{CD} is the surface area covered by a single CD host in CD SAMs.

$$C_{eff,max} = \frac{3}{2A_{CD}N_{AV}\bar{r}_o} \quad (9)$$

$C_{eff,max}$ scales with $\bar{r}_0{}^{-1}$ and therefore the effective concentration at the surface is much less dependent on $\bar{r}_0$ than in solution ($C_{eff} \approx \bar{r}_0{}^{-3}$). Consequently, the approximation of $C_{eff,max}$, based on a range of $\bar{r}_0$ gives a relatively narrow range of $C_{eff,max}$ values (0.20 to 0.50 M, see Supporting Information). Analogous to the solution case (see above) we chose to use the lower limit of $C_{eff,max}$ (0.20 M) for the fitting of the SPR titration curves.[41]

SPR curves were fitted to this model in a least squares optimization routine using $K_{i,s}$ as a variable and fixed values for $K_{i,l}$ (4.6×10^4 M^{-1}) and $C_{eff,max}$ (0.20 M). The SPR angle change, $\Delta\alpha$, was considered linearly dependent on the surface coverage of adsorbed guest and was calculated using eq 10.[37]

$$\Delta\alpha_{calcd} = \frac{[\mathbf{1}\cdot CD_s] + [\mathbf{1}\cdot (CD_s)_2] + [\mathbf{1}\cdot CD_s\cdot CD_l]}{[CD_s]_{tot}} \times \Delta\alpha_{max} \quad (10)$$

Results obtained by fitting the SPR curves using the sequential binding model are given in Table 2. The values for $K_{i,s}$ obtained for different concentrations of CD in solution are within the same order of magnitude and in good agreement with the previously obtained binding constant for the interaction of acetamidoadamantane with SAMs of **3**.[19] These results confirm that the concept of sequential binding interpreted in terms of C_{eff} and $K_{i,s}$ is also applicable to the interaction of **1** with CD SAMs. Comparison of the values for $K_{i,s}$ and K_{LM} indicate that fitting of the SPR curves using the sequential binding model gave a better understandable result for the interaction of **1** with the CD SAMs than the Langmuir fittings. By using the sequential binding model, the difference found in the binding constants for the divalent binding of **1** in solution and at CD SAMs can be explained in terms of effective concentrations; the effective concentration as experienced by monovalently bound **1** at CD SAMs is 2 orders of magnitude higher compared to the corresponding complex in solution with dimer **2**.[42]

Calculation of the complete speciation showed that the total concentration of surface-confined species at any point of the titration curves consisted for over 99% of $\mathbf{1}\cdot(CD)_2$, indicating that the intramolecular binding to the surface is dominant over the intermolecular binding. This can be explained by the fact that in all cases $C_{eff} \gg [CD_l]_{tot}$. Consequently, the observed binding constant for the interaction of **1** to CD SAMs is related to the intrinsic binding constants at the surface, $K_{i,s}$, and the maximum effective concentration at the surface, $C_{eff,max}$, as stated in eq 11.

$$K_{LM} = C_{eff,max}(K_{i,s})^2 \quad (11)$$

Apart from the statistical factor, eq 11 is similar to eq 1, the formula for the calculation of K for a divalent interaction in solution. Both divalent binding in solution and at surfaces can therefore be interpreted in terms of an effective concentration and intrinsic binding constants, and the relation between di- and monovalent binding is given by the simple eqs 1 and 11.

Conclusions

A significant difference in binding affinity of up to 3 orders of magnitude was observed for the divalent interaction of a bis-(adamantyl)-modified guest molecule **1** with CD dimer **2** in solution compared to the corresponding divalent interaction at CD SAMs. This difference in binding affinity was rationalized

(41) Alternatively, analogous to ref 35, $C_{eff,max}$ can be approximated from macrocyclization theory to be $13 \times 0.0245 = 0.32$ M, taking into account the accessibility of approximately 13 CD cavities with an effective concentration of 0.0245 M when assuming 30 rotatable bonds (see ref 30b).

(42) The apparently smaller error margins for $K_{i,s}$ compared to K_{LM} stem purely from the treatment of the data with divalent and monovalent models, respectively. To affirm this, under the experimental conditions employed here, there is a clear mathematical relationship between the two parameters, as given in eq 11.

by considering the divalent binding to consist of two sequential binding steps that can be expressed in terms of intrinsic binding constants and an effective concentration. Modeling indicated that this methodology is viable for the studied divalent binding interactions both in solution and at CD SAMs. By approximation of the effective concentration, intrinsic binding constants were obtained that gave a good correlation with experimentally determined values. The difference in binding affinity for the divalent interaction in solution with dimer **2** compared to the divalent interaction at CD SAMs was shown to originate mainly from a difference in effective concentration, which is 2 orders of magnitude higher at the CD SAMs. These differences in effective concentration in solution and at SAMs should be taken into account when analyzing multivalent binding at surfaces, as it can give rise to significant differences in binding compared to solution studies.

The methodology presented in this paper can easily be expanded to higher order multivalent binding and in principle allows the interpretation of any multivalent binding, whether in solution or at a surface, once the intrinsic binding constant for the corresponding monovalent interaction and the effective concentration are known.[43] The former is often readily available from literature and otherwise easily determined. The latter can be roughly estimated using the approaches presented above.

We envision that the current understanding of multivalent interactions as presented in this paper, combined with the more qualitative studies reported previously,[7,8] will provide a solid basis for the rational use of multivalency in nanoconstruction. The study presented here indicates that the effective concentration at SAMs is much less sensitive to changes in the spacer length compared to the effective concentration in solution. For this reason high affinity interactions at SAMs can be achieved with molecules containing limited directionality with respect to their guest moieties, and this can be taken advantage of in the design of multivalent guest molecules for the interaction with SAMs. The interaction between **1** and CD SAMs has already shown to be well suitable for this end. With the use of soft and probe lithographic techniques patterns of **1** at CD SAMs could be created that were stable in aqueous solution.[8]

Acknowledgment. We are grateful to the Council for Chemical Sciences of The Netherlands Organization for Scientific Research (NWO-CW) (A. M.: CW-programmasubsidie 700.98.305; T. A.: grant number 97041) and to the Ministero dell'Istruzione, Università, Ricerca (MIUR) (FIRB Project RBNEO19H9K: Manipolazione molecolare per macchine nanometriche) for financial support and to Dr. J. J. Michels for the synthesis of the EDTA-tethered CD dimer **2**.

Supporting Information Available: Estimation of $\bar{r}_0$ and derivation of eq 9. This material is available free of charge via the Internet at http://pubs.acs.org.

JA0317168

(43) A general model for multivalent binding on surfaces will be presented: Huskens, J.; Mulder, A.; Auletta, T.; Nijhuis, C. A.; Ludden, M. J. W.; Reinhoudt, D. N. *J. Am. Chem. Soc.* **2004**, *126*, 6784−6797.